Journal of Environmental Chemical Engineering 10 (2022) 107346

Contents lists available at ScienceDirect

Journal of Environmental Chemical Engineering

journal homepage: www.elsevier.com/locate/jece

3D imprinted superhydrophobic polyvinylidene fluoride/carbon black membrane for membrane distillation with electrochemical cleaning evaluation

N.A. Zakaria [a], S.Q. Zaliman [a], C.P. Leo [a,*], A.L. Ahmad [a], B.S. Ooi [a], Phaik Eong Poh [b]

[a] School of Chemical Engineering, Engineering Campus, Universiti Sains Malaysia, 14300 Nibong Tebal, Pulau Pinang, Malaysia
[b] Chemical Engineering Discipline, School of Engineering, Monash University Malaysia, Jalan Lagoon, 47500 Bandar Sunway, Selangor, Malaysia

ARTICLE INFO

Editor: V. Victor

Keywords:
PVDF
Membrane distillation
Carbon black
Superhydrophobic
Electrochemical cleaning

ABSTRACT

Although membrane distillation (MD) operates efficiently with different types of feed, the membrane could be wetted by synthetic surfactants and natural amphiphiles. In this work, carbon black was used to improve the surface hydrophobicity of the polyvinylidene fluoride (PVDF) membrane produced through 3D imprinting. PVDF membranes blended with 2–5 wt% of carbon black showed PVDF characteristic peaks and interactions with carbon black in Fourier transform infrared spectra. The presence of carbon black in the dope solution caused the length of finger-like voids to reduce but the membrane thickness to increase. The pore size increased by adding 2 or 3 wt% of carbon black. A higher amount of carbon black resulted in reduced pore size and porosity due to pore blockage by carbon black. Nevertheless, carbon black particles increased the surface roughness to form a superhydrophobic surface without using any hydrophobic agent. Although the superhydrophobic PVDF/carbon black membrane showed similar permeate flux to the neat PVDF membrane in MD, it could be electrochemically cleaned within 4 min to restore its permeate flux after wetting by the salt solution containing surfactant. The membrane could be cleaned by hypochlorite (OCl^-) and hypochlorous acid (HOCl) or metal hydroxides produced in electrochemical cleaning.

1. Introduction

Freshwater scarcity is a growing problem throughout the world due to climate change and pollution. This crisis leads to the development of different desalination technologies, including membrane distillation (MD). MD has been widely investigated since this emerging technology requires lower energy than reverse osmosis (RO). The other merits offered by MD include high rejection of non-volatile organic compounds, low operating temperature, and pressure with a small footprint [1]. MD even can be operated using brine solution as the feed since only water vapor passes through the hydrophobic porous membrane under the temperature difference between feed and permeate [2]. The hydrophobic porous membrane can be prepared through phase inversion or electrospinning of polymer solution. There are several types of polymer commonly used to prepare hydrophobic porous membranes, such as polyvinylidene fluoride (PVDF), polypropylene (PP), polyimide (PI), and polytetrafluoroethylene (PTFE) [3–5]. Different nanomaterials and templates were further applied to create roughness at the nanoscale, resulting superhydrophobic surface that can minimize wetting and fouling in membrane distillation [5–8].

Carbonaceous nanomaterials have been extensively used in the preparation of porous membranes for MD. Carbon nanotubes (CNT) have been long studied as the additives of porous polymeric membranes in MD because their surface can be functionalized with hydrophobic groups. Fan et al. [9] produced CNT hollow fiber membrane by sintering polyvinyl butyral/CNT hollow fiber membranes at 1000 °C, then modifying using 1 H, 1 H, 2 H, 2 H-perfluorooctyltriethoxysilane. A superhydrophobic surface with a water contact angle near 168° was attained after silanation, improving the permeate flux (25.5 kg m^{-2} h^{-1}) and antifouling properties in MD. The flux decline at 15% was further eliminated when the membrane was used as the cathode at 5.0 V. Wang et al. [10] spray-coated CNTs in PVA on PVDF membrane, then modified the composite membrane with 1 H,1 H,2 H,2 H-perfluorodecyltriethoxysilane. A water contact angle near 180° was recorded without affecting the permeate flux in MD compared to the neat PVDF membrane. Without modification, CNTs were commonly

* Corresponding author.
E-mail address: chcpleo@usm.my (C.P. Leo).

https://doi.org/10.1016/j.jece.2022.107346
Received 11 December 2021; Received in revised form 31 January 2022; Accepted 6 February 2022
Available online 9 February 2022
2213-3437/© 2022 Elsevier Ltd. All rights reserved.

incorporated into the electrospun membrane to attain a superhydrophobic surface. Tijing et al. [11] incorporated CNTs into polyvinylidene fluoride-co-hexafluoropropylene nanofiber membranes, which were prepared using electrospinning. The water contact angle on the membranes was significantly increased from 149 ± 1.21° to 158.5 ± 1.42° due to the improvement of surface roughness. The membrane pore size reduced significantly from 0.58 ± 0.01 μm to 0.29 ± 0.1 μm, but the permeation flux increased to 24–29.5 LMH. PVDF electrospun nanofiber membrane coated with CNTs under hot-press showed similar results. Superhydrophobic surface with a water contact angle of 159.3 ° formed and permeate flux was improved to 28.4 kg m^{-2} h^{-1} [12]. Essalhi et al. [13] compared CNTs and graphene oxide (GO) as the additives in the electrospun PVDF membranes. Superhydrophobic membranes formed using either CNTs or GO at a loading of 0.25 wt%, but an extremely high permeate flux of 74.7 kg m^{-2} h^{-1} was only achieved when dual-layered membranes were produced with polysulfone as the top or bottom layer.

Similarly, graphene improved the electrospun PVDF-co-hexafluoropropylene (HFP) membrane to attain a superhydrophobic surface with a contact angler larger than 162° and a permeate flux of 22.9 L m^{-2} h^{-1} in air-gap membrane distillation (AGMD) as reported by Woo et al. [14]. Using graphene as filler, Tittle et al. [5] had also studied the effect of laser patterning towards membrane characteristics. The superhydrophobic surface formed when the membrane was patterned with a spacing of 1/72 in using laser power higher than 4%. The membrane with a water contact angle of 176 ° and a roll-off angle of 0.61 ± 0.3 ° achieved a permeate flux of 10 kg m^{-2} h^{-1} in AGMD. Huang et al. [15] coated CNTs on the electrospun PVDF membrane through hot-pressing at 150 °C. The water contact angle was increased from 131.6° to 152.1°, promoting the water permeate flux to 0.65 kg m^{-2} h^{-1} using solar MD system. Dastbaz et al. [16] modified the PVDF-HFP/GO hollow fiber membranes using octadecyltrichlorosilane to form a superhydrophobic surface with a water contact angle as high as 162°. The liquid entry pressure (LEP) was significantly enhanced by silane modification even the pore size and porosity grew after incorporating GO. More importantly, the modified membrane showed consistent salt rejection in a long operation of MD, up to 250 h. Recently, Kujawa et al. [3] spray-coated the sonicated or oxidized single-walled carbon nanohorn (CNH) in alcohol on a PVDF membrane. Hydrophilic and superhydrophobic surfaces could be formed, depending on the pretreatment. The superhydrophobic PVDF/CNF membrane exhibited 14–27% improvement of permeate flux compared to the neat membrane.

The use of carbonaceous materials was extended into the electrochemical cleaning of membranes. Abid et al. [17] coated the polymeric spacer with carbon ink containing graphene nanoplates and placed it on the PVDF membrane. During microfiltration of sodium alginate suspension, hydrogen bubbles were generated in the membrane module with a graphite electrode (anode) at −0.81 V to clean the membrane. In the aerobic wastewater treatment system, CNT hollow fiber membrane recovered 92% of flux under electrochemical assistance between 0.5 and 1.5 V [18]. Graphene hydrogel membrane with bovine serum albumin (BSA) fouling recovered its flux up to 99.0 ± 0.1% after electrochemical cleaning at 1.0 V for 60 min using 0.1 M Na_2SO_4 solution [19]. Electrochemical cleaning at 2.5 V also eliminated the dyes accumulated on the PVDF membrane with double layer coating of CNT and graphene prepared through vacuum filtration [20]. In addition to membranes modified with carbon nanomaterials, the conductive polypyrrole membrane supported on stainless steel could be electrochemically cleaned at 2.0 V after being fouled by sodium alginate, BSA or humic acid [21]. Biofouling on polyethersulfone (PES) ultrafiltration was further abolished using platinum electrodes in the seawater electrolysis into chlorine gas and sodium hydroxide (NaOH). However, the electrochemical cleaning of superhydrophobic membrane wetted in membrane distillation has not been studied.

The low-cost carbon black has been recently used to fabricate superhydrophobic membranes. The carbon black was modified using hydrophobic silane before blending into the PVDF membrane [22] mixed with polyurethane before being filter-coated on the PVDF membrane [23]. A facile method is introduced in this work to produce superhydrophobic PVDF membrane using carbon black without hydrophobic modification. In this work, carbon black was used to build hierarchical roughness on PVDF membranes with micro-roughness imprinted after peeling off from the non-woven support used in phase inversion. The modified membranes were characterized and tested in membrane distillation. The membranes fouled by surfactant were electrochemically cleaned to restore the surface hydrophobicity.

2. Materials and methods

2.1. Materials

PVDF (Solef ® 6010 powder) from Solvay Solexis (France) was used as the polymer to prepare the dope solution. The solvent, N-methyl-2-pyrrolidone (NMP) (>99.5%), was supplied by Merck (Darmstadt, Germany) and directly used without any pretreatment procedure. The carbon black was acquired from the School of Material and Mineral Resources, Universiti Sains Malaysia. Sodium chloride (NaCl) (>99.5%) supplied by Sigma-Aldrich was used to prepare the saline solution for the membrane distillation test and electrochemical cleaning. Sodium dodecyl sulfate (SDS) (>97%) supplied by Sigma-Aldrich was used as a surfactant to wet membranes.

2.2. Synthesis and modification of membrane

PVDF membrane was first prepared through phase inversion with a template as described in another work [24]. NMP was heated up to 60 °C. Then, PVDF (15 wt%) was gradually added into the solvent and stirred for 6 h to prepare the dope solution of the neat PVDF membrane. In addition, 2, 3, and 5 wt% of carbon black were added to the dope solution of PVDF-C2, PVDF-C3, and PVDF-C5 membranes, respectively. The dope solution was sonicated for 1 h to remove bubbles. The dope solution was then cast on the non-woven support fixed on a glass plate. The casting was conducted at a casting gap of 400 μm using an automated casting machine (XB320D, Beijing Jiahang Technology Co. Ltd., China). The wet film was submerged in a coagulation bath of distilled water for 24 h to form a PVDF membrane through phase inversion. Then, the solidified PVDF membrane was dried for another 24 h at room temperature. The solidified PVDF membranes were peeled off from the non-woven support to achieve 3D imprinting of the microstructure on the non-woven surface [24].

2.3. Membrane characterization

The surface morphology and cross-section of the neat PVDF and PVDF-carbon black membranes were studied using a scanning electron microscope (SEM, TM3000, Hitachi, Japan). Fourier transform infrared (FTIR) spectra were collected from 600 cm^{-1} to 3800 cm^{-1} using spectroscopy (Nicolet iS10, Thermo Scientific, USA). The mean pore size of membranes was analyzed using a porometer (Porolux 1000, IB-FT GmbH, Germany). Before measuring the mean pore size, the samples were wetted in Porefil for 30 min. Membrane porosity was determined by measuring wet weight and dry weight. Wet weight was obtained by immersing 3 cm × 1 cm area of membrane in 2-butanol for 2 h, while dry weight was obtained by drying the wet membrane at 40 °C in an oven. Then, the overall porosity, ε (%), was calculated using the following equation.

$$\varepsilon = \frac{m_b/\rho_b}{m_b/\rho_b + m_m/\rho_m} \times 100\% \quad (1)$$

where m_b is the weight of 2-butanol absorbed by the membrane (g), m_m is the weight of dry membrane (g), ρ_b is the density of 2-butanol (0.81 g/cm^3), ρ_m is the density of the PVDF (1.78 g/cm^3). The contact angle

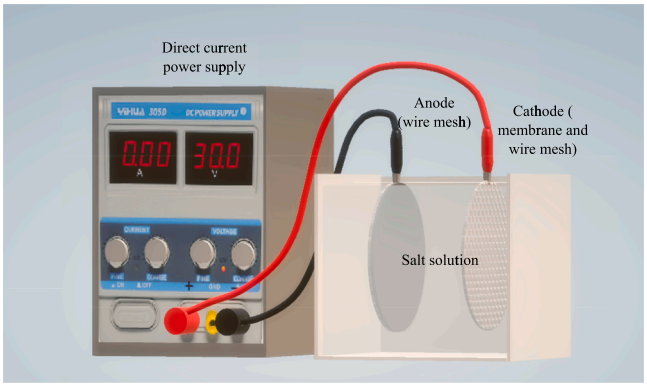

Fig. 1. Electrochemical cleaning setup of PVDF-C3 membrane using stainless steel mesh as anode, membrane clamped with stainless steel mesh as cathode and 2 wt% of NaCl solution as electrolyte.

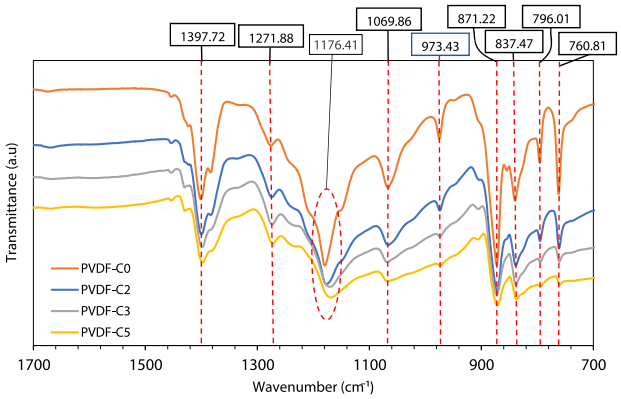

Fig. 2. FTIR spectra of the PVDF membranes with different carbon black contents.

measurement was conducted using the image of a water droplet (10 μl) placed on the membrane surface. The electronic microscope (1000X Electronic Digital Microscope Handheld USB Magnifier) was used to capture the water droplet images. Using ImageJ software, the average water contact angle was measured from 3 replicates of measurement for each membrane sample. Meanwhile, the sliding angle was measured using a contact angle goniometer (LSA 200, Lauda). The surface roughness was measured using an atomic force microscope (AFM, Hitachi SPA 300HV). The membrane conductivity was measured using a multimeter (Projecta, DT-830B Digital Multimeter). The membranes incorporated with carbon black were further characterized using a potentiostat (Metrohm, μStat 300, Spain). Cyclic voltammetry (CV) test was conducted using phosphate buffer solution (0.05 M) with a scanning range of −0.5 to + 1.2 V with a scanning rate of 0.01 V/s.

2.4. Direct contact membrane distillation (DCMD) performance test

The membranes fabricated in this work were tested in a direct contact membrane distillation (DCMD) system as described in our previous work [25]. The membrane sample with an effective area of 0.001 m^2 acting as the separation barrier was placed in a membrane module to separate the hot feed from the cold permeate. The saline solution containing 35 g/L of NaCl at 60 ± 2° was used as hot feed while the distilled water at 20 ± 2° was used as cold permeate. Both streams circulated counter-currently into the membrane module at 500 mL/min using two peristaltic pumps. For DCMD experiments, the superhydrophobic surface imprinted by the non-woven support was used to prevent fouling by the feed. The salt rejection was determined by measuring the salt concentration of feed and permeate solutions. The permeate flux, J (kg/m^2·h) during DCMD was calculated using the following equation

$$J = \frac{\Delta W}{A \quad \Delta t} \tag{2}$$

where ΔW is the distillation water mass difference (kg), A is the effective area of flat-sheet membrane (m^2), and Δt is the sampling time (h). The rejection coefficient, R (%), was calculated using:

$$R \quad (\%) = \left[1 - \quad \frac{C_p}{C_f}\right] \quad \times 100 \tag{3}$$

where C_p is the NaCl concentration of the permeate (g/L) and C_f is the NaCl concentration of the feed (g/L).

2.5. Electrochemical cleaning

For electrochemical cleaning, the membrane samples were statically fouled by immersing the membrane in the salt solution containing surfactant [24]. The fouling solution contains 3.5 wt% of NaCl and 0.15 mM of sodium dodecyl sulfate (SDS). The membrane samples were immersed into the fouling solution for 5 h and then dried at room temperature for 24 h. The dried membrane samples were subsequently cleaned electrochemically [25]. The external electric field was supplied by a direct current power supply (Nice Power SPS-305, 0–5 A, 0–30 V). The anode is the wire mesh with a diameter of 15 mm placed 1 cm from the cathode, which is another piece of wire mesh clamped together with the PVDF-carbon black membrane as shown in Fig. 1. NaCl solution (2 wt%) was used in the electrochemical cleaning process conducted at 2 V for 1, 2 or 4 min. The water contact angle on the membrane samples before and after electrolysis was measured as described previously. The membrane samples were also tested in membrane distillation before and after electrochemical cleaning.

3. Results and discussion

3.1. Membrane characteristics

The PVDF membrane turned into black color after incorporating 2–5 wt% of carbon black. The images for the neat PVDF and the PVDF membrane incorporated with 2 wt% carbon black are shown in Fig. S1. The membranes were further characterized to understand the difference in their characteristics. The FTIR spectra of the neat PVDF membrane (PVDF-C0) and PVDF membranes with varied carbon black content (PVDF-C2, PVDF-C3, PVDF-C5) are shown in Fig. 2. All the PVDF membranes in this work exhibited PVDF peaks, namely 760.81, 796.01, 871.22, 973.43, 1069.86, and 1176.41 cm^{-1} [26–28]. The peak at 871.22 cm^{-1} represents C-C-C symmetrical stretching [29], while peaks at 1271.88 cm^{-1} and 1397.72 cm^{-1} represent C-F stretching vibrations [30,31]. These membranes displayed a broader peak at 1176.41 cm^{-1} and shifted to peaks at 837.47 and 1069.86 cm^{-1}, indicating the interfacial interaction (physical adsorption or weak chemical bonding) between PVDF and carbon particles [11,32].

The surface morphology and cross-section of the neat PVDF and PVDF membranes modified with varied carbon content from 0 wt% to 5 wt% are shown in Fig. 3. All membranes possess asymmetric structures with interconnected polymer molecules that form symmetric pores on the top, as reported elsewhere [24]. Fig. 3(a) i, (a) ii, (b) i, (b) ii, (c) i, (c) ii, (d) i, and (d) ii show the surface of membranes with the imprinted roughness of the non-woven support. The 3D weave pattern of non-woven support was imprinted on the membrane surface after phase inversion and drying. The 3D structure was clearly shown in the embedded figure of Fig. 3(a) i. The porous structure, pore size, and surface roughness exhibited by all types of membranes in this work were influenced by the solvent exchange rate in the coagulation bath. The finger-like voids formed because of the fast solvent exchange rate. Even the carbon content increased, all membranes exhibited similar

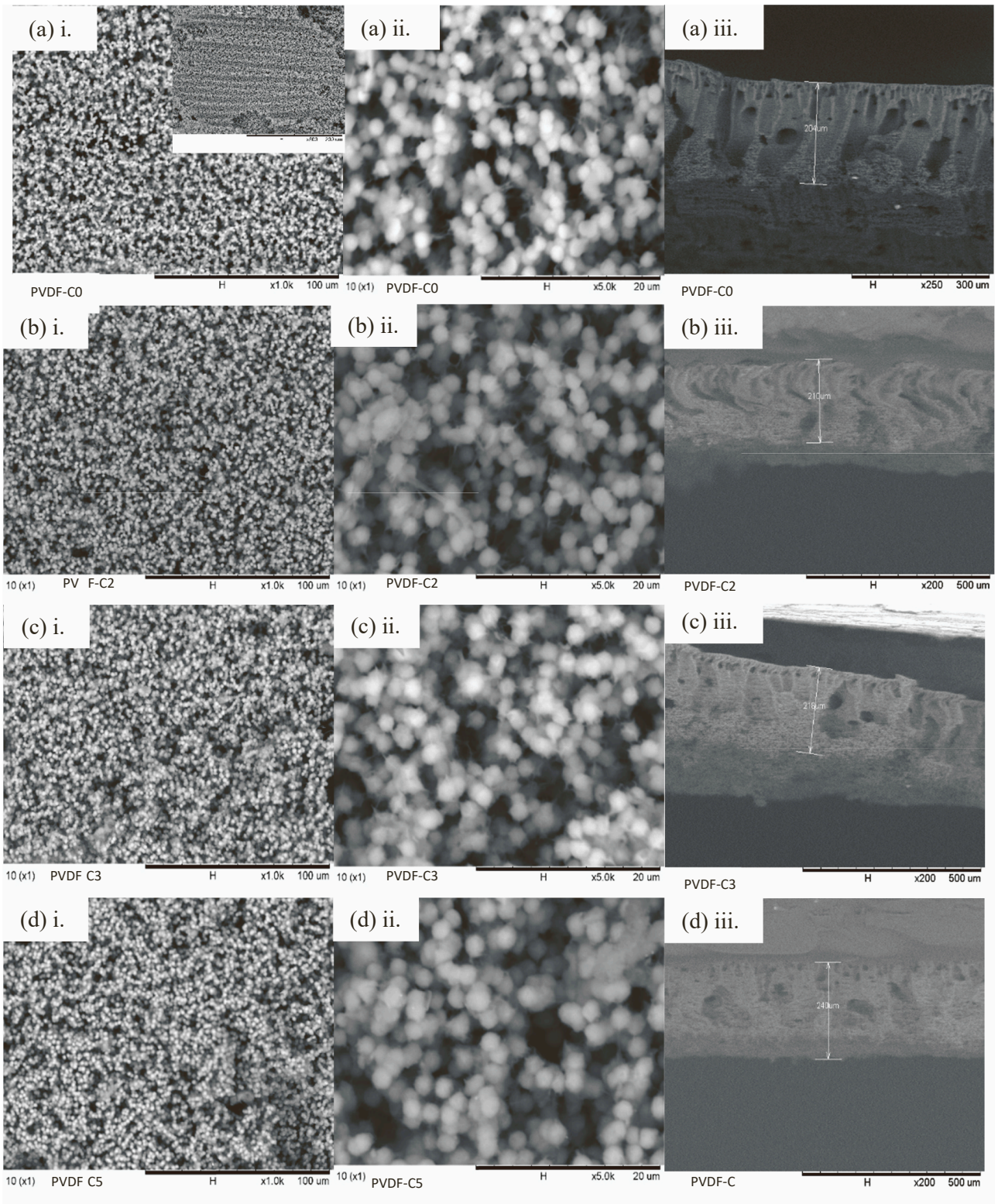

Fig. 3. SEM images showing the surface and cross-section of (a) the neat PVDF membrane (PVDF-C0), and the PVDF membranes with varied carbon black contents: (b) 2 wt% (PVDF-C2), (c) 3 wt% (PVDF-C3) and (d) 5 wt% (PVDF-C5).

morphology to the neat PVDF, as shown by the SEM images (Fig. 3(b), (c), and (d)). The finger-like voids reduced in size at the same time, indicating the reduced demixing rate. The PVDF membranes blended with CNTs reported by others [27] showed a similar asymmetric structure with finger-like voids. However, the increasing carbon content reduced the surface pore size and extended the finger-like voids due to the fast-demixing rate during phase inversion. Graphene oxide nanosheets blended into PVDF-HFP hollow fiber membrane caused the thickness growth as they migrated to the surface [16]. A small amount of graphene oxide nanosheet also induced the increment of pore size, but pore size reduction was observed by increasing the amount of graphene oxide nanosheet. The membrane thickness was further determined using

Table 1
The characteristics of the neat PVDF membrane and the PVDF membrane with different carbon black contents.

Membrane	Carbon black content (wt%)	Thickness (μm)	Mean pore size (μm)	Porosity (%)	Water contact angle (°)	Sliding angle (°)	Mean roughness (μm)	Conductivity (1/Ωm)
PVDF-C0	0	204	0.17 ± 0.02	67.7 ± 0.4	141.6 ± 0.6	44.0 ± 0.3	0.0778	–
PVDF-C2	2	210	0.22 ± 0.01	64.3 ± 0.2	143.6 ± 1.9	33.6 ± 0.4	0.1121	0.0327
PVDF-C3	3	218	0.22 ± 0.06	61.1 ± 0.4	152.0 ± 0.7	10.1 ± 0.2	0.1669	0.3022
PVDF-C5	5	240	0.17 ± 0.03	57.8 ± 0.2	160.2 ± 0.4	9.9 ± 0.1	0.1703	0.3617

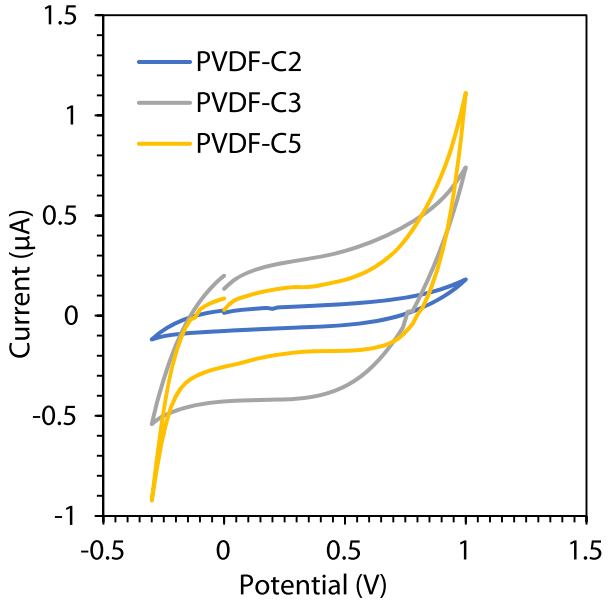

Fig. 4. Cyclic voltammogram for PVDF-Carbon membrane with (a) 2 wt% (PVDF-C2), (b) 3 wt% (PVDF-C3) and (c) 5 wt% (PVDF-C5) of carbon content.

SEM images in Fig. 3. The membrane thickness increased significantly as the carbon content was increased from 2 wt% to 5 wt% compared to the neat PVDF membrane (PVDF-C0). The addition of carbon black could increase the viscosity of the membrane solution, resulting in thickness growth under blade casting. Similarly, the viscosity of the PVDF dope solution was raised by graphene and caused the growth of membrane thickness, as reported by others [33].

The mean pore size and porosity of the neat PVDF membrane the PVDF membranes blended with carbon black were further measured and summarized in Table 1. The incorporation of carbon black caused the pore size to increase, as shown in SEM images (Fig. 3). The pore size increased slightly at the low carbon black loading because the carbon black disturbed the thermodynamic stability of the dope solution and resulted in a fast demixing rate in phase inversion. PVDF-C3 membrane exhibited the largest mean pore size of 0.22 μm and porosity of 61.3%. As the carbon content further increased to 5 wt% in the PVDF-C5 membrane, the mean pore size and porosity decreased. Similar changes in pore size of PVDF membranes were observed by others [34] when the loading of MWCNTs was excessively increased. The observation could be related to the viscosity changes of membrane dope solution. As the carbon content grew, the membrane dope solution became viscous and caused a delay in phase inversion and limited the pore growth [35]. The blending of graphene oxide into PVDF-HFP membranes also resulted in similar changes in pore size [16]. The reduction of pores size at high loading as the graphene oxide blocked the pores.

The water contact angle and sliding angle of the neat PVDF membrane and PVDF membranes modified with varied carbon black content are tabulated in Table 1, and the water droplet images are shown in Fig. S2. The neat PVDF showed the lowest water contact angle among the fabricated membranes with a value of 141.6 ± 0.6° and high sliding angle, which is 44.0 ± 0.3°. The high water contact angle value exhibited by neat PVDF (PVDF-C0) is because of the imprinting effects of the non-woven support, as shown in the SEM image (Fig. 3(a) i) [22]. In addition to surface chemistry, the surface roughness could increase the surface hydrophobicity of PVDF membranes. The surface roughness of PVDF membranes could also be created using dual-coagulation baths to attain near superhydrophobic surfaces instead of templates, but excessive ethanol was required for the demixing process [7]. The water contact angle values of PVDF/carbon black membranes increased, but their sliding angle reduced when the carbon content was raised. The highest water contact angle with a value of 160.15° was obtained as the carbon content reached 5 wt% (PVDF-C5). The existence of carbon black particles increased the surface roughness sufficiently to form a superhydrophobic surface without using any hydrophobic agent in this work. The mean roughness of PVDF/carbon black membrane increased as shown in Table 1. The past studies [7,16] usually required hydrophobic agents, especially silanes, to create superhydrophobic PVDF membrane prepared from phase inversion even though nanoparticles were added. Unlike those PVDF membranes prepared through phase inversion, the electrospun PVDF membranes with superhydrophobic surfaces could be easily fabricated with carbonaceous nanoparticles [11].

The membrane conductivity increased with the increasing carbon black content as shown in Table 1. Hence, a very low current was recorded in the CV curves of PVDF-C2, PVDF-C3, and PVDF-C5 membranes. The CV curves of PVDF membranes incorporated with carbon black are shown in Fig. 4. The CV curve of PVDF-C2 membrane was thin and narrow within the whole scanning range due to the limited redox properties. With the increasing carbon black content in PVDF-C3 and PVDF-5 membranes, the CV curves became wider. The conductivity was slightly improved, as reported by others [21].

3.2. *Direct contact membrane distillation (DCMD) performance test*

The neat PVDF membrane (PVDF-C0) and the modified PVDF membranes with varied carbon black content (PVDF-C2, PVDF-C3, PVDF-C5) were tested in DCMD. Fig. 5 shows the permeate flux of water vapor transferred from the hot feed solution at 60 °C counter-currently through the membrane into cold permeate at 20 °C. All membranes were tested for 3 h at a flow rate 500 mL/min for both hot and cold sides. The permeate flux for all membranes was only slightly reduced after 3 h of operation, while the NaCl rejection was maintained at ~99%. The slight changes in permeate flux could be related to the minor wetting of membranes due to the use of highly hydrophobic membranes. Moreover, the partial pressure suppression of water vapor as the feed concentration did not increase significantly in 3 h [34,35]. As illustrated in Fig. 5, PVDF-C0, PVDF-C2, and PVDF-C3 membranes attained similar permeate flux near 15.0 L/m^2 h. However, PVDF-C5 membrane only gained a very low permeate flux around 5.0 L/m^2 h. The permeate flux of the PVDF-C5 membrane (Fig. 5(d)) was the lowest among membranes fabricated in this work. It exhibited the smallest pore size and the lowest porosity after incorporating the highest loading of carbon black, as summarized in Table 1. Similar outcomes were reported in other studies, where the permeate flux declined when the carbon content was increased. The flux decline was mainly caused by the reduction of pore size and porosity (Table 1) [13,35,37].

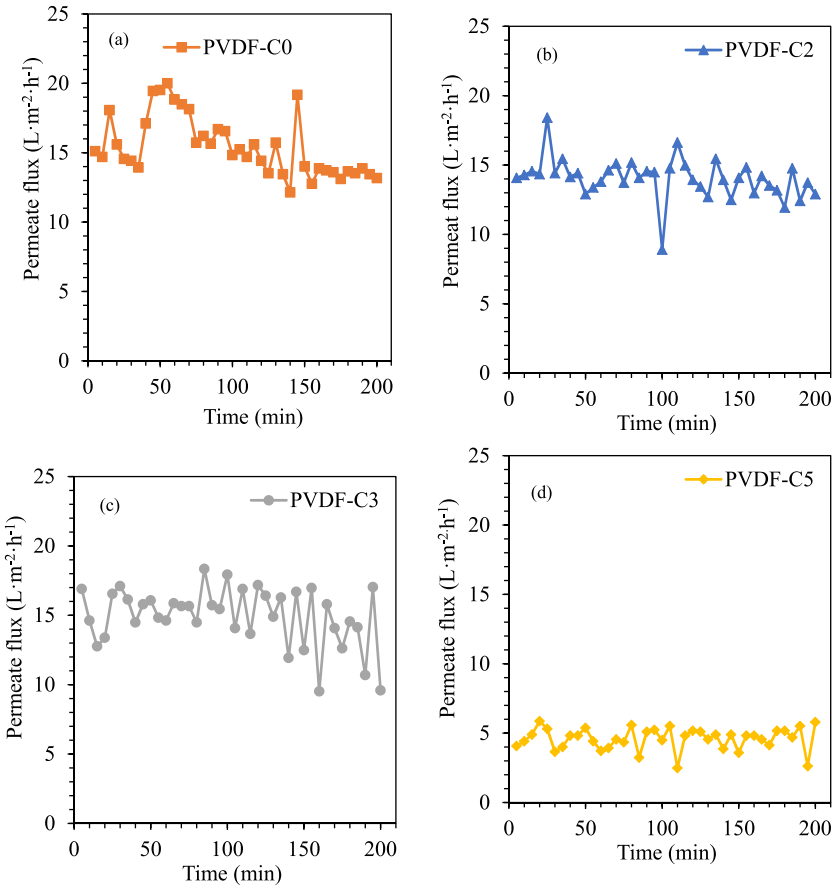

Fig. 5. The water permeability of (a) the neat PVDF membrane (PVDF-C0) and PVDF membranes with (b) 2 wt% (PVDF-C2), (c) 3 wt% (PVDF-C3) and (d) 5 wt% (PVDF-C5) of carbon black.

Table 2
The water contact angle measurement on the PVDF-C0 and PVDF-C3 membranes with different time of electrochemical cleaning process.

Electrochemical cleaning duration (min)	Membrane	Water contact angle (°)
0	PVDF-C0E	96.1 ± 0.1
	PVDF-C3E	132.1 ± 0.4
1	PVDF-C0E1	118.9 ± 0.6
	PVDF-C3E1	138.9 ± 0.7
2	PVDF-C0E2	129.3 ± 0.9
	PVDF-C3E2	141.5 ± 0.9
4	PVDF-C0E4	134.9 ± 0.4
	PVDF-C3E4	143.9 ± 0.5

3.3. Membrane wetting and electrochemical cleaning

In the long operation of MD, the wetting of superhydrophobic membranes still occurs due to the presence of synthetic surfactants and natural amphiphiles [38,39]. Hence, it is important to understand the wetting and cleaning of superhydrophobic PVDF membranes. In the subsequent study for membrane wetting and electrochemical cleaning, the neat PVDF membrane and PVDF membrane with 3 wt% of carbon black (PVDF-C3) were selected. The efficiency of electrochemical cleaning was evaluated through water contact angle measurement before and after the electrochemical cleaning process with different cleaning durations, as shown in Table 2. The membranes were immersed in a salt solution containing 3.5 wt% of NaCl and 0.3 mM of surfactant (SDS) for 5 h. The cleaned membranes were dried at room temperature for 24 h before measuring the water contact angle. The color of membrane samples remained the same before and after electrochemical cleaning. As seen in Table 2, the water contact angle on PVDF-C3 membrane without electrochemical cleaning dropped from 152.2 ± 0.7° to 132.1 ± 0.4°. The water contact angle on PVDF-C0 membrane dropped even more significantly from 141.6 ± 0.6° to 96.1 ± 0.1°. The wetting occurred due to the hydrophobic interaction between hydrophobic tails of SDS surfactant with the membrane surface [40]. Subsequently, a hydrophilic layer covered the membrane surface because of the orientation of the hydrophilic head of the surfactant to face outward. The electrostatic repulsion of surfactant by the PVDF membrane with a negatively charged surface was further reduced by NaCl in the solution [40,41]. The PVDF-C0 membrane with a hydrophobic surface was more severely wetted by SDS surfactant compared to the PVDF-C3 membrane with a superhydrophobic surface. The wetting was promoted by the direct contact between the surfactant and the hydrophobic surface of the PVDF-C0 membrane. At Cassie-Baxter state, the air captured on the superhydrophobic surface of the PVDF-C3 membrane reduced the direct contact and wetting. The water contact angle on the PVDF-C3 membrane could be partially restored after electrochemical cleaning with increasing duration from 1 min to 4 min. The cleaning of PVDF-C0 membrane was less successful, leading to a restored water contact angle of 134.9 ± 0.4° only. Besides working as the electrolyte, the presence of NaCl possibly caused the formation of hypochlorite (OCl^-) and hypochlorous acid (HOCl) to clean the surfactant accumulated on the membrane surface [42]. Moreover, the stainless steel mesh could produce insoluble ferric hydroxides at a low concentration that is sufficient to induce coagulation [43]. The foulants could be removed through electrostatic absorption followed by coagulation. This method is beneficial for other foulants such as dyes.

Based on the cleaning results, the PVDF-C0 and PVDF-C3 membranes were tested in the MD system. With the hot feed containing 35 g/L of

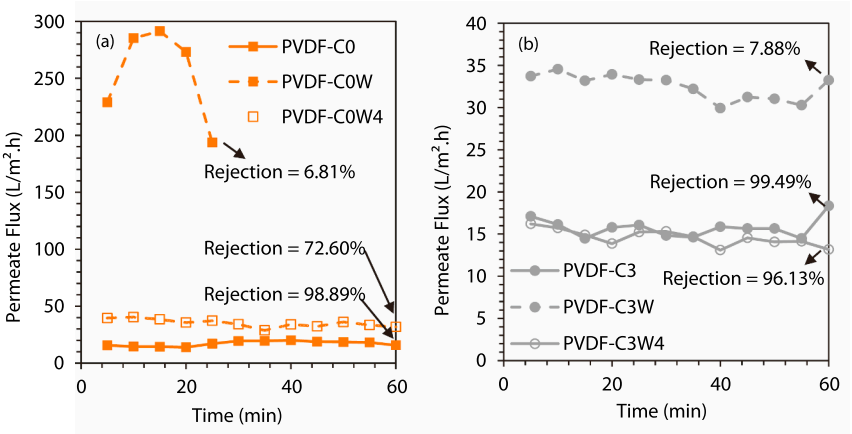

Fig. 6. The permeability of (a) neat PVDF (PVDF-C0) and (b) PVDF membrane modified with 3 wt% of carbon black (PVDF-C3) using NaCl solution (solid line with solid marker), NaCl/0.15 mM of surfactant solution (dotted line with solid marker) and NaCl solution using PVDF-C0 and PVDF-C3 membrane after 4 min of electrochemical cleaning (dotted line with no fill marker).

NaCl and 0.3 mM of SDS [24], the membranes (PVDF-C0W and PVDF-C3W) were significantly wetted. The permeate flux of the PVDF-C0W membrane increased nearly to 300 L/m^2 h and then reduced as the hot feed ran out after 20 min (Fig. 6(a)). Instead of water vapor permeation, feed permeation through the membrane occurred since the salt rejection was only 6.81%. Meanwhile, the permeate flux for the PVDF-C3W membrane kept increasing and capped near to 35 L/m^2 h after 1 h (Fig. 6(b)). The highest permeate flux was recorded using PVDF-C3W with only about 7.88% of NaCl rejection. The membrane wetting was induced by both hydrophobic interactions (nonpolar tails) and electrostatic interactions (polar head) with surfactant [40]. PVDF membrane surface is negatively charged to repel surfactant, but the electrostatic repulsion was reduced by the salt [41,44]. The wetted membranes were then electrochemically cleaned for 4 min before being MD tested in MD again with only 35 g/L of NaCl in distilled water as the hot feed stream. As shown in Fig. 6(a), the cleaned PVDF membrane (PVDF-C0W4) achieved higher permeate flux than the neat PVDF membrane without wetting (PVDF-C0), but the salt rejection of the PVDF-C0W4 membrane was low, only 72.6%. The permeate flux of the cleaned PVDF-C3W4 membrane returned near to the permeate flux of PVDF-C3 membrane without wetting (~15.0 L/m^2 h), and the NaCl rejection was maintained at 96.13%. The membrane rejection had not been fully restored compared to the fresh PVDF-carbon membrane. The membrane cleaning should be further improved to attain salt rejection of more than 99%, and in-situ cleaning should be studied in future work.

4. Conclusions

The FTIR spectra of PVDF membranes blended with carbon black showed PVDF characteristic peaks and interactions with carbon black. Adding carbon black into the dope solution of PVDF membranes caused changes in membrane morphology, pore size, porosity, thickness and wettability. The finger-like voids were shortened, but the membrane thickness was increased due to the reduction of the demixing rate during phase inversion. The pore size increased by adding 2 or 3 wt% of carbon black. However, the membrane pore size and porosity reduced significantly when 5 wt% of carbon black was added into the PVDF dope solution. The reduction could be related to pore blockage by carbon black. Nevertheless, carbon black particles increased the surface roughness to form a superhydrophobic surface without using any hydrophobic agent in this work. Although the superhydrophobic PVDF/carbon black membrane showed similar permeate flux to the neat PVDF membrane in MD, it could be electrochemically cleaned within 4 min after wetting by the salt solution containing surfactant. The cleaned membrane showed a restored permeate flux in MD as the surfactant was removed by hypochlorite (OCl^-) and hypochlorous acid (HOCl) or metal hydroxides produced in the electrochemical cleaning setup.

CRediT authorship contribution statement

N.A. Zakaria: Investigation, Methodology, Writing – original draft. **S.Q. Zaliman:** Investigation. **C.P. Leo:** Conceptualization, Methodology, Writing – review & editing, Supervision, Funding acquisition. **A.L. Ahmad:** Resources. **B.S. Ooi:** Funding acquisition. **Phaik Eong Poh:** Investigation.

Declaration of Competing Interest

The authors declare that they have no known competing financial interests or personal relationships that could have appeared to influence the work reported in this paper.

Acknowledgments

The authors would like to acknowledge the Ministry of Higher Education Malaysia (LRGS/1/2018/USM/01/1/4; 203/PJKIMIA/67215002) to provide financial support for conducting this work. 1) This work is also the output of the ASEAN IVO (http://www.nict.go.jp/en/asean_ivo/index.html) project, IoT System for Water Reuse in Developing Cities, and financially supported by NICT (http://www.nict.go.jp/en/index.html).

Appendix A. Supplementary material

Supplementary data associated with this article can be found in the online version at doi:10.1016/j.jece.2022.107346.

References

[1] Y.C. Woo, S.H. Kim, H.K. Shon, L.D. Tijing, Introduction: Membrane Desalination Today, Past, and Future, Elsevier Inc., 2018.
[2] N.N.R. Ahmad, W.L. Ang, C.P. Leo, A.W. Mohammad, N. Hilal, Current advances in membrane technologies for saline wastewater treatment: a comprehensive review, Desalination 517 (2021), 115170, https://doi.org/10.1016/j.desal.2021.115170.
[3] J. Kujawa, M. Zięba, W. Zięba, S. Al-Gharabli, W. Kujawski, A.P. Terzyk, Carbon nanohorn improved durable PVDF membranes – the future of membrane distillation and desalination, Desalination 511 (2021), 115117, https://doi.org/10.1016/j.desal.2021.115117.
[4] J. Huang, Y. Hu, Y. Bai, Y. He, J. Zhu, Solar membrane distillation enhancement through thermal concentration, Energy 211 (2020), 118720, https://doi.org/10.1016/j.energy.2020.118720.
[5] C.M. Tittle, D. Yilman, M.A. Pope, C.J. Backhouse, Robust superhydrophobic laser-induced graphene for desalination applications, Adv. Mater. Technol. 3 (2018) 1–10, https://doi.org/10.1002/admt.201700207.

[6] H.F. Tan, W.L. Tan, N. Hamzah, M.H.K. Ng, B.S. Ooi, C.P. Leo, Membrane distillation crystallization using PVDF membrane incorporated with TiO2 nanoparticles and nanocellulose, Water Sci. Technol. Water Supply 20 (2020) 1629–1642, https://doi.org/10.2166/ws.2020.068.
[7] H.F. Tan, W.L. Tan, B.S. Ooi, C.P. Leo, Superhydrophobic PVDF/micro fibrillated cellulose membrane for membrane distillation crystallization of struvite, Chem. Eng. Res. Des. 170 (2021) 54–68, https://doi.org/10.1016/j.cherd.2021.03.027.
[8] L.N. Nthunya, L. Gutierrez, L. Lapeire, K. Verbeken, N. Zaouri, E.N. Nxumalo, B. B. Mamba, A.R. Verliefde, S.D. Mhlanga, Fouling-resistant PVDF nanofibre membranes for the desalination of brackish water in membrane distillation, Sep. Purif. Technol. 228 (2019), 115793, https://doi.org/10.1016/j.seppur.2019.115793.
[9] X. Fan, Y. Liu, X. Quan, H. Zhao, S. Chen, G. Yi, L. Du, High desalination permeability, wetting and fouling resistance on superhydrophobic carbon nanotube hollow fiber membrane under self-powered electrochemical assistance, J. Membr. Sci. 514 (2016) 501–509, https://doi.org/10.1016/j.memsci.2016.05.003.
[10] Y. Wang, M. Han, L. Liu, J. Yao, L. Han, Beneficial CNT intermediate layer for membrane fluorination toward robust superhydrophobicity and wetting resistance in membrane distillation, ACS Appl. Mater. Interfaces 12 (2020) 20942–20954, https://doi.org/10.1021/acsami.0c03577.
[11] L.D. Tijing, Y.C. Woo, W.G. Shim, T. He, J.S. Choi, S.H. Kim, H.K. Shon, Superhydrophobic nanofiber membrane containing carbon nanotubes for high-performance direct contact membrane distillation, J. Membr. Sci. 502 (2016) 158–170, https://doi.org/10.1016/j.memsci.2015.12.014.
[12] K.K. Yan, L. Jiao, S. Lin, X. Ji, Y. Lu, L. Zhang, Superhydrophobic electrospun nanofiber membrane coated by carbon nanotubes network for membrane distillation, Desalination 437 (2018) 26–33, https://doi.org/10.1016/j.desal.2018.02.020.
[13] M. Essalhi, M. Khayet, S. Tesfalidet, M. Alsultan, N. Tavajohi, Desalination by direct contact membrane distillation using mixed matrix electrospun nanofibrous membranes with carbon-based nanofillers: a strategic improvement, Chem. Eng. J. 426 (2021), 131316, https://doi.org/10.1016/j.cej.2021.131316.
[14] Y.C. Woo, L.D. Tijing, W.G. Shim, J.S. Choi, S.H. Kim, T. He, E. Drioli, H.K. Shon, Water desalination using graphene-enhanced electrospun nanofiber membrane via air gap membrane distillation, J. Membr. Sci. 520 (2016) 99–110, https://doi.org/10.1016/j.memsci.2016.07.049.
[15] J. Huang, Y. Hu, Y. Bai, Y. He, J. Zhu, Novel solar membrane distillation enabled by a PDMS/CNT/PVDF membrane with localized heating, Desalination 489 (2020), 114529, https://doi.org/10.1016/j.desal.2020.114529.
[16] A. Dastbaz, J. Karimi-Sabet, H. Ahadi, Y. Amini, Preparation and characterization of novel modified PVDF-HFP/GO/ODS composite hollow fiber membrane for Caspian Sea water desalination, Desalination 424 (2017) 62–73, https://doi.org/10.1016/j.desal.2017.09.030.
[17] H.S. Abid, B.S. Lalia, P. Bertoncello, R. Hashaikeh, B. Clifford, D.T. Gethin, N. Hilal, Electrically conductive spacers for self-cleaning membrane surfaces via periodic electrolysis, Desalination 416 (2017) 16–23, https://doi.org/10.1016/j.desal.2017.04.018.
[18] Y. Yang, S. Qiao, R. Jin, J. Zhou, X. Quan, A novel aerobic electrochemical membrane bioreactor with CNTs hollow fiber membrane by electrochemical oxidation to improve water quality and mitigate membrane fouling, Water Res. 151 (2019) 54–63, https://doi.org/10.1016/j.watres.2018.12.012.
[19] J. Sun, C. Hu, B. Wu, J. Qu, Fouling mitigation of a graphene hydrogel membrane electrode by electrical repulsion and in situ self-cleaning in an electro-membrane reactor, Chem. Eng. J. 393 (2020), 124817, https://doi.org/10.1016/j.cej.2020.124817.
[20] G. Wei, Y. Zhao, J. Dong, M. Gao, C. Li, Electrochemical cleaning of fouled laminar graphene membranes, Environ. Sci. Technol. Lett. 7 (2020) 773–778, https://doi.org/10.1021/acs.estlett.0c00617.
[21] Y. Zhang, T. Wang, J. Meng, J. Lei, X. Zheng, Y. Wang, J. Zhang, X. Cao, X. Li, X. Qiu, J. Xue, A novel conductive composite membrane with polypyrrole (PPy) and stainless-steel mesh: fabrication, performance, and anti-fouling mechanism, J. Membr. Sci. 621 (2021), 118937, https://doi.org/10.1016/j.memsci.2020.118937.
[22] S.S. Ray, M. Gandhi, S.S. Chen, H.M. Chang, C.T.N. Dan, H.Q. Le, Anti-wetting behaviour of a superhydrophobic octadecyltrimethoxysilane blended PVDF/recycled carbon black composite membrane for enhanced desalination, Environ. Sci. Water Res. Technol. 4 (2018) 1612–1623, https://doi.org/10.1039/c8ew00451j.
[23] G. Cao, Y. Wang, C. Wang, S.H. Ho, A dually prewetted membrane for continuous filtration of water-in-light oil, oil-in-water, and water-in-heavy oil multiphase emulsion mixtures, J. Mater. Chem. A 7 (2019) 11305–11313, https://doi.org/10.1039/c9ta01889a.
[24] G.H. Teoh, J.Y. Chin, B.S. Ooi, Z.A. Jawad, H.T.L. Leow, S.C. Low, Superhydrophobic membrane with hierarchically 3D-microtexture to treat saline water by deploying membrane distillation, J. Water Process Eng. 37 (2020), 101528, https://doi.org/10.1016/j.jwpe.2020.101528.
[25] N. Hamzah, C.P. Leo, Fouling prevention in the membrane distillation of phenolic-rich solution using superhydrophobic PVDF membrane incorporated with TiO2 nanoparticles, Sep. Purif. Technol. 167 (2016) 79–87, https://doi.org/10.1016/j.seppur.2016.05.005.
[26] X. Liao, Y. Wang, Y. Liao, X. You, L. Yao, A.G. Razaqpur, Effects of different surfactant properties on anti-wetting behaviours of an omniphobic membrane in membrane distillation, J. Membr. Sci. 634 (2021), 119433, https://doi.org/10.1016/j.memsci.2021.119433.
[27] B.S. Lalia, F.E. Ahmed, T. Shah, N. Hilal, R. Hashaikeh, Electrically conductive membranes based on carbon nanostructures for self-cleaning of biofouling, Desalination 360 (2015) 8–12, https://doi.org/10.1016/j.desal.2015.01.006.
[28] R. Gregorio, Determination of the α, β, and γ crystalline phases of poly(vinylidene fluoride) films prepared at different conditions, J. Appl. Polym. Sci. 100 (2006) 3272–3279, https://doi.org/10.1002/app.23137.
[29] H. Bai, X. Wang, Y. Zhou, L. Zhang, Preparation and characterization of poly (vinylidene fluoride) composite membranes blended with nano-crystalline cellulose, Prog. Nat. Sci. Mater. Int. 22 (2012) 250–257, https://doi.org/10.1016/j.pnsc.2012.04.011.
[30] A. Khalid, A.A. Al-Juhani, O.C. Al-Hamouz, T. Laoui, Z. Khan, M.A. Atieh, Preparation and properties of nanocomposite polysulfone/multi-walled carbon nanotubes membranes for desalination, Desalination 367 (2015) 134–144, https://doi.org/10.1016/j.desal.2015.04.001.
[31] F.A. Abuilaiwi, T. Laoui, M. Al-Harthi, M.A. Atieh, Modification and functionalization of multiwalled carbon nanotube (MWCNT) via fischer esterification, Arab. J. Sci. Eng. 35 (2010) 37–48.
[32] K. Ke, P. Pötschke, D. Jehnichen, D. Fischer, B. Voit, Achieving β-phase poly (vinylidene fluoride) from melt cooling: Effect of surface functionalized carbon nanotubes, Polymer 55 (2014) 611–619, https://doi.org/10.1016/j.polymer.2013.12.014.
[33] N. Awanis Hashim, Y. Liu, K. Li, Stability of PVDF hollow fibre membranes in sodium hydroxide aqueous solution, Chem. Eng. Sci. 66 (2011) 1565–1575, https://doi.org/10.1016/j.ces.2010.12.019.
[34] C. Athanasekou, A. Sapalidis, I. Katris, E. Savopoulou, K. Beltsios, T. Tsoufis, A. Kaltzoglou, P. Falaras, G. Bounos, M. Antoniou, P. Boutikos, G.E. Romanos, Mixed matrix PVDF/graphene and composite-skin PVDF/graphene oxide membranes applied in membrane distillation, Polym. Eng. Sci. 59 (2019) E262–E278, https://doi.org/10.1002/pen.24930.
[35] T.L.S. Silva, S. Morales-Torres, J.L. Figueiredo, A.M.T. Silva, Multi-walled carbon nanotube/PVDF blended membranes with sponge- and finger-like pores for direct contact membrane distillation, Desalination 357 (2015) 233–245, https://doi.org/10.1016/j.desal.2014.11.025.
[37] J. Ravi, M.H.D. Othman, Z.S. Tai, T. El-badawy, T. Matsuura, T.A. Kurniawan, Comparative DCMD performance of hydrophobic-hydrophilic dual-layer hollow fibre PVDF membranes incorporated with different concentrations of carbon-based nanoparticles, Sep. Purif. Technol. 274 (2021), 118948, https://doi.org/10.1016/j.seppur.2021.118948.
[38] T. Horseman, Y. Yin, K.S. Christie, Z. Wang, T. Tong, S. Lin, Wetting, scaling, and fouling in membrane distillation: state-of-the-art insights on fundamental mechanisms and mitigation strategies, ACS ES&T Eng. 1 (2021) 117–140, https://doi.org/10.1021/acsestengg.0c00025.
[39] Y.Z. Tan, S. Velioglu, L. Han, B.D. Joseph, L.G. Unnithan, J.W. Chew, Effect of surfactant hydrophobicity and charge type on membrane distillation performance, J. Membr. Sci. 587 (2019), 117168, https://doi.org/10.1016/j.memsci.2019.117168.
[40] N.G.P. Chew, S. Zhao, C.H. Loh, N. Permogorov, R. Wang, Surfactant effects on water recovery from produced water via direct-contact membrane distillation, J. Membr. Sci. 528 (2017) 126–134, https://doi.org/10.1016/j.memsci.2017.01.024.
[41] D. Hou, Z. Yuan, M. Tang, K. Wang, J. Wang, Effect and mechanism of an anionic surfactant on membrane performance during direct contact membrane distillation, J. Membr. Sci. 595 (2020), 117495, https://doi.org/10.1016/j.memsci.2019.117495.
[42] P. Taylor, I. Kabda, T. Ölmez-hanc, O. Tünay, Electrocoagulation applications for industrial wastewaters: a critical review, Environ. Technol. Rev. (2012) 37–41, https://doi.org/10.1080/21622515.2012.715390.
[43] M.A. Ahangarnokolaei, H. Ganjidoust, B. Ayati, Optimization of parameters of electrocoagulation/ flotation process for removal of acid red 14 with mesh stainless steel electrodes, J. Water Reuse Desalin. 8 (2018) 278–292, https://doi.org/10.2166/wrd.2017.091.
[44] S. Paria, K.C. Khilar, A review on experimental studies of surfactant adsorption at the hydrophilic solid-water interface, Adv. Colloid Interface Sci. 110 (2004) 75–95, https://doi.org/10.1016/j.cis.2004.03.001.